Journal of Steroid Biochemistry & Molecular Biology 124 (2011) 112–120

Contents lists available at ScienceDirect

Journal of Steroid Biochemistry and Molecular Biology

journal homepage: www.elsevier.com/locate/jsbmb

HL005—A new selective PPARγ antagonist specifically inhibits the proliferation of MCF-7

Weiqiang Lu[a], Peng Che[a], Yanyan Zhang[a], Honglin Li[a], Shien Zou[b], Jin Zhu[a], Jing Deng[a], Xu Shen[a,c], Hualiang Jiang[a,c], Jian Li[a,*], Jin Huang[a,*]

[a] Shanghai Key Laboratory of Chemical Biology, School of Pharmacy, East China University of Science and Technology, 130 Meilong Road, Shanghai 200237, China
[b] The Obstetrics and Gynecology Hospital of Fudan University, Shanghai 200011, China
[c] Drug Discovery and Design Center, Shanghai Institute of Materia Medica, Chinese Academy of Sciences, Shanghai 201203, China

ARTICLE INFO

Article history:
Received 2 November 2010
Received in revised form 26 January 2011
Accepted 28 January 2011

Keywords:
Peroxisome proliferator-activated receptor-γ
Selective antagonist
Anticancer
Apoptosis

ABSTRACT

Peroxisome proliferator-activated receptor-γ (PPARγ) is a nuclear transcription factor which is involved in many diseases, such as diabetes, inflammation, dyslipidemia, hypertension, and cancer. Recently, there are many reports showing that PPARγ agonists have preclinical and clinical anticancer activity, with relatively few reports on anticancer effects of PPARγ antagonists. From our compound library, a novel 3-thiazolinone-modified benzoic acid derivative HL005 is found as PPARγ selective ligand through SPR analysis (K_D = 0.21 μM), yeast two-hybrid results suggest that HL005 antagonize the potent PPARγ agonist rosiglitazone-induced recruitment of the coactivator for PPARγ (IC_{50} = 7.97 μM). Different from the most reported PPARγ antagonist, HL005 can inhibit the proliferation of MCF-7 cell line in a concentration-dependent manner and induce cell cycle arrest at G2/M phase, other than interference with cell adhesion. In order to study the binding mode of this compound, three derivatives are synthesized to get more detail about the structure–activity relationship, molecular docking and the NMR spectra indicate that similar to most PPARγ ligand, the carboxylic acid group is an important moiety for HL005 and contributes strong interaction with PPARγ.

1. Introduction

Peroxisome proliferator activated receptors (PPARs) are ligand-activated transcription factors with pleiotropic effects on cell fate and metabolism [1–3], among the various subtypes of PPARs (PPARα, PPARβ/δ and PPARγ), PPARγ is the best characterized receptor in humans. Past studies identified PPARγ as an essential mediator for maintenance of whole body insulin sensitivity [4] and thus PPARγ had developed into an important therapeutic target in treatment of type 2 diabetes. Up to now, PPARγ is found expressed not only in the adipose tissue but also in the immune system organ, adrenals and small intestine, and because of its anti-proliferative, pro-apoptotic and differentiation promoting activities, PPARγ has been intensively evaluated as a target for anti-cancer therapy in preclinical models [5–10]. Either a deficiency in PPARγ expression or overexpression of PPARγ enhanced risk for carcinogenesis [11]. The early research find that selective PPARγ modulators have potential effects to suppress carcinogenesis in experimental models and induce the differentiation of human tumorigenic cells, such as troglitzone and ciglitazone exhibit antitumor activity in human cancer cell lines containing prostate [12], breast [13], colon [14], thyroid [15], lung [16] and pituitary carcinoma [17]. So, it is still great challenge for us to identify new chemical classes of PPARγ binders and study the interaction mode between the binder and PPARγ.

PPARγ works as a ligand-activated transcription factor, after the PPARγ/RXR (retinoid-X receptor) heterodimer binds to PPRE (peroxisome proliferator response element) on promoter regions of target genes, coactivator proteins such as SRC-1 and CBP are recruited to this complex to modulate gene transcription [18]. Different PPARγ ligands appear to be able to recruit different coactivators, which may explain differences in the biological activity for different ligands [19,20]. Such as PPARγ agonists – troglitazone and 15d-PGJ2 showed anti-neoplastic effects by inducing apoptosis [21,22], while ciglitazone caused an arrest in the G2/M phase of cell cycle [23], and PPARγ antagonists GW9662 and T0070907 caused cell death through interference with cell adhesion [24–26].

Recently, the discovery of potential druggable PPAR ligand is mainly through two approaches, one is PPAR pan agonists, and another is SPPARM (selective PPAR modulator) [19], PPARγ is the PPAR subtype that has seen the most activity in identification and study of SPPARM. Compared to the PPARγ agonists, few reports focused on the discovery of PPARγ

* Corresponding authors.
E-mail address: huangjin@ecust.edu.cn (J. Huang).

0960-0760/$ – see front matter © 2011 Elsevier Ltd. All rights reserved.
doi:10.1016/j.jsbmb.2011.01.019

antagonists work as anticancer agent. In the current work, we report a novel 3-thiazolinone-modified benzoic acid derivative, 5-((Z)-5-(3-chloro-5-ethoxy-4-hydroxybenzylidene)-3-methyl-4-oxothiazolidin-2-ylideneamino)-2-chlorobenzoic acid (HL005), which is confirmed to be a potent PPARγ specific antagonist by employing the surface plasmon resonance (SPR) technology and yeast two-hybrid assay. Three derivatives (HL006–HL008) are designed and synthesized to verify the binding mode between the protein and compounds. Anti-proliferation shows HL005 can significantly inhibit the proliferation of MCF-7 cancer cell and caused cell cycle arrest at G2/M phase.

2. Materials and methods

2.1. Materials

All solvents and reagents were purchased commercially and were used without further purifications. The restriction and modification enzymes in this work were purchased from NEB. The affinity columns and lower molecular weight (LMW) marker were from Amersham Pharmacia Biotech, isopropyl β-D-thiogalactopyranoside (IPTG) was from Promega. Yeast nitrogen base without amino acids, yeast related mediums were all from Sigma. Dulbecco's modified Eagle's medium (DMEM), RPMI1640 and MEM medium were from GibcoBRL, and fetal bovine serum (FBS) was from HyClone. The other chemicals were purchased from Sigma, Lancaster, Acros and Shanghai Chemical Reagent Company. HCT-116, Du-145, H446, HeLa, PNAC-1, HepG2, Tca-8113, LS-174T, MCF-7, ZR-75-30 cell lines were purchased from The Cell Bank of Type Culture Collection of Chinese Academy of Sciences, Shanghai Institute of Cell Biology, Chinese Academy of Sciences.

2.2. Plasmids construction and protein expression

The PPARα-LBD (aa 199–468) and PPARδ-LBD (aa 28–477) were amplified by PCR from pSG–hPPARα (Provided by Dr. X. Lu, Shenzhen Chipscreen Biosciences Ltd.), pAdTrack–PPARδ (Provided by Dr. B. Vogelstein, Howard Hughes Medical Institute, USA) respectively, and then subcloned into vector pET15b to express the His-tagged fusion protein by standard method [27]. The plasmid pET15b–hPPARγ-LBD (aa 204–477) was kindly provided by Dr. J. Uppenberg, Department of Structural Chemistry, Pharmacia and Upjohn, Sweden.

Expression and purification of hPPARγ-LBD, PPARα-LBD and PPARδ-LBD proteins was carried out using the method with slight modifications as described [14]. The recombinant plasmids were transformed into BL21(DE3) *Escherichia coli* bacteria, and cells were grown in LB medium with 100 mg/L of ampicillin at 37 °C until an OD600 of 0.6, the expressions were induced by the addition of 0.5 mM of isopropyl β-D-thiogalactopyranoside (IPTG), and cells were harvested after induction for additional 5 h at 25 °C. The pellet was washed, frozen (overnight in an ultra-low-temperature), and then sonicated for 30 min on ice in buffer A (50 mM Tris–HCl, 0.5 M NaCl, 10 mM imidazole, pH 8.0). The lysed cells were centrifuged at 15,000 × *g* and 4 °C for 30 min. The supernatant was loaded onto a nickel–nitrilotriacetic acid (Ni–NTA) resin (Qiagen) column (1 mL) pre-equilibrated with binding buffer. After 2 h the column was washed with washing buffer A and buffer B (60 mM imidazole in buffer A), the protein of interest was eluted with 10 mL elution buffer (50 mM Tris–HCl, 0.5 M NaCl, 150 mM imidazole, pH 8.0). The fractions containing the target protein were identified by SDS–PAGE. Imidazole was removed by dialysis against the corresponding buffer (10 mM HEPES, 150 mM NaCl, 3 mM EDTA, pH 8.0). The proteins were concentrated with a 10-kDa cut-off membrane (Amicon) at 4 °C and the concentration was measured by the standard Bradford method.

2.3. Ligand binding assay

Binding affinity of compounds towards PPARγ-LBD, PPARδ-LBD and PPARα-LBD were assayed using a SPR-based Biacore 3000 instrument. N-hydroxysuccinimide (NHS), N-ethyl-N′-(3-dimethylaminopropyl) carbodiimide (EDC), and ethanolamine coupling reagents were used to immobilize the proteins to the sensor surface following a standard amine-coupling procedure. The proteins to be covalently bound to the matrix were diluted in 10 mM sodium acetate buffer (pH4.5) to a final concentration of 0.10 mg/ml. The baseline was equilibrated with a continuous flow of running buffer (10 mM HEPES, 150 mM NaCl, 3 mM EDTA, and 0.005% (v/v) surfactant P20) through the chip for 1–2 h. Different concentrations of compounds were injected into the channels at a flow rate of 30 μL min^{-1} for 60 s, followed by disassociation for 120 s. BIAevaluation software version 3.1 (Biacore) and the 1:1 Langmuir binding fitting model were used to determine the equilibrium dissociation constant (K_D) of compounds.

2.4. Yeast transformation, culture and α-galactosidase activity assay

The yeast strain AH109 was obtained from Clontech (Palo Alto, CA), and transformation was performed according to the lithium acetate method. Briefly, 500 ng of plasmid DNA (pGADT7–CBP and pGBKT7–PPARγ) was added to 50 μL of the competent cells and mixed with 36 μL of 1 M lithium acetate, 240 μL of 50% PEG3350 and 50 ng single-strain DNA at 30 °C for 30 min, followed by heat-shock (250 rpm) at 42 °C for 30 min. The mixture was subsequently spread on a drop-out-agar plate without leucine and tryptophan (SD–T$^-$L$^-$). The plate was incubated at 30 °C for 48 h for yeast growth and the PCR technique was used to confirm the successful transformation of the target gene.

The quantitative α-galactosidase activity assays were carried out using p-nitrophenyl α-D-galactopyranoside (PNP-α-Gal) as the substrate according to the Clontech manual. The α-galactosidase activity was calculated according to the following formula:

$$\alpha\text{-galactosidase activity[milliunits/(ml} \times \text{cell)]} = \mathrm{OD}_{410} \times V_f \times \frac{1000}{(\xi \times b) \times t \times V_i \times \mathrm{OD}_{600}}$$

where t is the elapsed time of incubation (min), V_f is the final volume of assay (200 μL), V_i equal to the volume of culture medium supernatant added (16 μL), OD_{600} is the optical density of overnight culture, $\xi \times b$ is the p-nitrophenol molar absorptivity at 410 nm × light path (cm) = 10.5 (ml/μmol; Yeast Protocols Handbook PT3024-1, Clontech).

2.5. In vitro cellular proliferation assay, apoptosis and cell cycle analysis

Du-145, LS-174T, HeLa and MCF-7 cells were cultured in EMEM medium supplemented with 10% fetal bovine serum, H446, Tca-8113 and ZR-75-30 cells were cultured in RPMI-1640 medium supplemented with 10% fetal bovine serum. HCT-116, HepG2 and PNAC-1 cell lines were cultured using DMEM medium supplemented with 10% fetal bovine serum. MTT assay [28] was used to evaluate the effect of compounds against HCT-116, Du-145, H446, HeLa, PNAC-1, HepG2, Tca-8118, Ls-174, MCF-7 and ZR-75-30 cells. Cells were seeded in 96-well plates with 5000 cells per well in the presence of certain concentration compounds solution. The solvent (DMSO) was added to control wells at equal volumes to those used

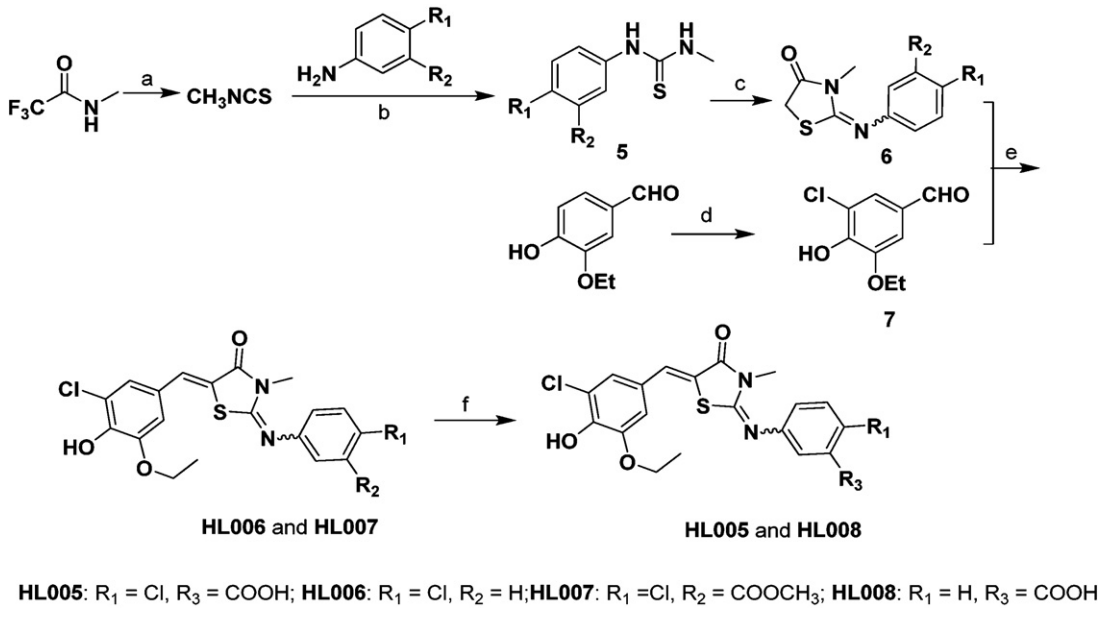

Scheme 1. Reagents and conditions: (a) CS_2, K_2CO_3, NaOH, CH_3CN; (b) CH_3CN, 25 °C; (c) CH_3COONa, EtOH, reflux; (d) Cl_2 (g) AcOH; (e) piperidine, EtOH, reflux; (f) LiOH, THF/CH_3OH = 3/1, 25 °C.

for the compounds. The plates were then incubated at 37 °C in a 5% CO_2-supplemented atmosphere. After incubation for 48 h, 20 μL of 5 mg/mL MTT was added and the plate was incubated for a further 4 h. Then the converted dye was dissolved in 100 μL of DMSO and the absorbance was measured at 570 nm, cell viabilities were calculated from the data of three wells. The wells with or without drugs were used as positive or negative controls.

MCF-7 cells (2 × 105 cells/well) were seeded in six-well plates and incubated overnight to allow cells to attach to the plate. After cells incubated with different concentrations of HL005 for 48 h, the adherent cells were detached with trypsin and the floating cells were then collected by centrifugation at 600 × *g*. After washing with pre-cooled PBS once, resuspended the cell pellet in 500 μl binding buffer containing 5 μl PI and 2.5 μl Annexin V (BD). Incubate the cell suspension in dark (room temperature) for 10 min, then inspect the stained cells with BD FACSCalibur and analyze the apoptosis data using BD CellQuest Pro software.

After treatment, the harvested cells were further washed twice with pre-cooled PBS and fixed in 75% ethanol at 4 °C for 3 h, and collected by centrifugation. Cells were resuspended with 500 μl PBS containing 100 mg/ml RNase A and incubated for 30 min at 37 °C, followed by filtration and staining with 0.05 mg/ml propidium iodide (PI) for 1 h. The suspensions were then analyzed by Becton Dichinson FACScan BD Biosciences, San Jose, CA. The percentage of cells in the G0/G1, S and G2/M phases of cell cycle was determined by their DNA contents and presented as fold of control.

2.6. Molecular docking simulation

To gain structural information for further structural optimization, the 3D binding models of HL005 to PPARγ ligand-binding domain (LBD) was generated based on the docking simulation. The crystal structure of a PPARγ-LBD complexed with TZD was retrieved from Protein Data Bank (PDB entry 2PRG) [29]. Molecular docking was performed using the FlexX program [30], which is a flexible docking method that uses an incremental construction algorithm to dock ligand into the active site. The ligand-binding pocket of PPARγ-LBD was defined as the residues enclosed within 6.5 Å radius around the bound ligand (TZD). After crystallographic water molecules and bound ligand were removed from the protein coordinates [31]. All charges were assigned to the protein using the BIOPOLYMER module of the Sybyl package (in mol2 format). The 3D structure of HL005 was constructed by Corina program [32] and formal charges were assigned to HL005 atoms. Standard parameters of the FlexX program were used during the molecular docking simulation, and the top 30 solutions ranked by *F*-score were retained and further stored in mol2 format.

2.7. ^{13}C NMR spectra

Samples for NMR measurements were prepared by dissolving the sodium salt of HL005 with and without protein in a solution (0.50 mL) of Tris buffer (20 mM Tris solved in D_2O, pH 8.0). The ^{13}C NMR 1D spectra were collected on a Bruker DRX-500 NMR spectrometer at 298 K with recycle delays of 3 s, and were recorded on a spectral width of 300 ppm.

2.8. Design and synthesis of compounds HL005–HL008

To validate binding model between HL005 and PPARγ-LBD based on the docking simulation, three more compounds HL006–HL008 were synthesized on the basis of structural feature of HL005.

Scheme 1 depicts the sequence of reactions that led to the preparation of compounds HL005–HL008. 1-Methyl-3-arylthiourea (**5**) were prepared by N-acylate with methyl isothiocyanate, which was synthesized from N-methyltrifluoroacetamide [33], then cycloaddition reaction between **5** and chloroacetic acid give the key intermediate **6**, subsequently, the target compounds HL006 and HL007 were obtained by **6** condensation with substituted benzaldehyde (**7**) in ethanol, the later was produced by chlorination of 3-ethoxy-4-hydroxybenzaldehyde [34]. Finally HL005 and HL008 were obtained by hydrolysis reaction using LiOH at room temperature.

Analytical thin-layer chromatography (TLC) was HSGF 254 (150–200 μm thickness, Yantai Huiyou Company, China). Yields were not optimized. Melting points were measured in capillary tube on a SGW X-4 melting point apparatus without correction. Nuclear magnetic resonance (NMR) spectra were given on a Brucker DRX-500 NMR (IS as TMS). Chemical shifts were reported in parts

per million (ppm, δ) downfield from tetramethylsilane. Proton coupling patterns were described as singlet (s), doublet (d), triplet (t), quartet (q), multiplet (m), and broad (br). Low- and high-resolution mass spectra (LRMS and HRMS) were given with electric (EI) produced by Finnigan MAT-95 spectrometer.

*2.8.1. Methyl 2-chloro-5-(3-methylthioureido)benzoate (**5a**)*

A solution of N-methyltrifluoroacetamide (1.27 g, 10 mmol), NaOH (0.8 g, 20 mmol), K_2CO_3 (4.15 g, 30 mmol) and CS_2 (2.4 mL, 40 mmol) in MeCN (20 mL) was stirred at 25 °C for 45 min. The reactive mixture was filtered, which was used in next step without purification [33]. To the above solution was added methyl 5-amino-2-chlorobenzoate (1.5 g, 8 mmol), the resulting solution was stirred overnight at 40 °C, poured into H_2O (40 mL), extracted with EtOAc. The combined organic layer was washed, dried, filtered and condensed. The residue was purified by flash column chromatography on silica gel, eluted with a mixture of EtOAc/petroleum ether (1:4, v/v), to afford **5a** (0.95 g, 46%) as a pale yellow solid: mp 172–174 °C; ^{1}H NMR ($CDCl_3$, 500 MHz): δ 3.11 (s, 3H), 3.92 (s, 3H), 7.36 (dd, 1H, J = 7.5 and 2.0 Hz), 7.47 (d, 1H, J = 7.5 Hz), 7.69 (d, 1H, J = 2.0 Hz).

*2.8.2. Methyl 5-(3-methyl-4-oxothiazolidin-2-ylideneamino)-2-chlorobenzoate (**6a**)*

A mixture of **7a** (0.93 g, 3.6 mmol), chloroacetic acid (0.7 g, 7.4 mmol), NaoAc (0.9 g, 11 mmol), and ethanol (30 mL) was refluxed under stirring for 12 h. The reaction mixture was concentrated under reduced pressure to approximately 10 mL, and then allowed to cool in ice and filtered, to afford **6a** (0.86 g, 80%) as a pale white solid: mp 101–102 °C; ^{1}H NMR ($CDCl_3$, 500 MHz): δ 3.32 (s, 3H), 3.86 (s, 2H), 3.95 (s, 3H), 7.07 (dd, 1H, J = 7.2 and 1.8 Hz), 7.44 (d, 1H, J = 7.2 Hz), 7.48 (d, 1H, J = 1.8 Hz).

2.8.3. 3-Chloro-5-ethoxy-4-hydroxybenzaldehyde (7) [34]

To a solution of 3-ethoxy-4-hydroxybenzaldehyde (6.0 g, 36 mmol) in glacial acetic acid (15 mL) was added chlorine gas through a glass tubing over 30 min (with a slow gas flow) at 25 °C. White solid product was collected by filtration, washed with 50 mL of hexane, and dried in vacuo to give **7** (3.1 g, 43%) as a pale white solid: mp 141–143 °C; ^{1}H NMR ($CDCl_3$, 500 MHz): δ 1.49 (t, 3H, J = 7.0 Hz), 4.22 (q, 2H, J = 7.0 Hz), 6.45 (s, 1H), 7.29 (d, 1H, J = 1.7 Hz), 7.47 (d, 1H, J = 1.7 Hz), 9.76 (s, 1H).

2.8.4. Methyl 5-((Z)-5-(3-chloro-5-ethoxy-4-hydroxybenzylidene)-3-methyl-4-oxothiazolidin-2-ylideneamino)-2-chlorobenzoate (HL007)

A mixture of **6a** (0.26 g, 1 mmol), **7** (0.2 g, 1 mmol), piperidine (0.1 g, 1.2 mmol), and ethanol (5 mL) was refluxed under stirring for 15 h. The reaction mixture was poured into H_2O, yellow solid product was collected by filtration, washed with water and the mixture of EtOAc/petroleum ether (1:8, v/v), and dried in vacuo to give HL007 (0.42 g, 96%) as a yellow solid: mp 116–117 °C; ^{1}H NMR ($CDCl_3$, 500 MHz: δ 1.45 (t, 3H, J = 7.0 Hz), 3.41 (s, 3H), 3.92 (s, 3H), 4.13 (q, 2H, J = 7.0 Hz), 6.80 (d, 1H, J = 1.7 Hz), 7.68 (m, 2H), 7.49 (m, 2H), 7.61 (s, 1H); EI-MS m/z 480 (M^+, 100%); HRMS (EI) m/z calcd $C_{21}H_{18}N_2O_5SCl_2$ (M^+) 480.0313, found 480.0308.

2.8.5. 5-((Z)-5-(3-chloro-5-ethoxy-4-hydroxybenzylidene)-3-methyl-4-oxothiazolidin-2-ylideneamino)-2-chlorobenzoic acid (HL005)

A mixture of HL007 (0.22 g, 0.5 mmol) and LiOH (45 mg, 1 mmol) in THF: methanol (3:1, v/v, 10 mL) was stirred at room temperature for 15 h. The resulting solution was acidified to pH 2 using 1 N HCl and added water (50 mL). Yellow solid product was collected by filtration, washed with water and the mixture of EtOAc/petroleum ether (1:2, v/v), and dried in vacuo to give HL005 (0.12 g, 57%) as a yellow solid: mp 261–262 °C; ^{1}H NMR (DMSO-d_6, 500 MHz): δ 1.33 (t, 3H, J = 7.0 Hz), 3.31 (s, 3H), 4.09 (q, 2H, J = 7.0 Hz), 7.08 (d, 1H, J = 1.7 Hz), 7.15 (d, 1H, J = 1.7 Hz), 7.22 (dd, 1H, J = 8.5 and 2.5 Hz), 7.44 (d, 1H, J = 2.5 Hz), 7.58 (d, 1H, J = 8.5 Hz), 7.68 (s, 1H); ^{13}C NMR (DMSO-d_6, 500 MHz): δ 166.7 (COOH), 166.2 (C=O), 152.1 (C=N), 148.3, 147.0, 145.5, 132.8, 132.2, 130.5, 127.8, 125.8, 125.3, 123.7, 123.4, 121.0, 119.1, 114.0, 67.5, 65.2, 30.3, 15.4; EI-MS m/z 466 (M^+, 100%); HRMS (EI) m/z calcd $C_{20}H_{16}N_2O_5SCl_2$ (M^+) 466.0157, found 466.0157.

Table 1
Kinetic parameters for the binding of our compounds to PPARγ-LBD.

Compound	PPARγ-LBD			
	k_{on}[M^{-1} S^{-1}]	k_{off} [S^{-1}]	K_D [M]	χ^2
HL005	0.85×10^2	1.75×10^{-5}	2.06×10^{-7}	4.38
HL006	NA	NA	NA	NA
HL007	NA	NA	NA	NA
HL008	8.49×10^3	5.32×10^{-2}	6.27×10^{-6}	0.46

2.8.6. Sodium salt of HL005

A mixture of HL005 (85 mg, 0.18 mmol) and NaOH (7.2 mg, 0.18 mmol) in methanol (5 mL) was stirred at room temperature for 1 h at which time the reaction was complete by TLC analysis (10% methanol/chloroform, silica gel). The reaction solution was concentrated under reduced pressure, gave orange solid product.

2.8.7. (5Z)-5-(3-chloro-5-ethoxy-4-hydroxybenzylidene)-2-(4-chlorophenylimino)-3-methylthiazolidin-4-one (HL006)

In the same manner as described for HL007. mp 209–210 °C; ^{1}H NMR ($CDCl_3$, 500 MHz): δ 1.46 (t, 3H, J = 7.0 Hz), 3.46 (s, 3H), 4.12 (q, 2H, J = 7.0 Hz), 6.80 (d, 1H, J = 1.7 Hz), 6.96 (d, 2H, J = 8.5 Hz), 7.04 (d, 1H, J = 1.7 Hz), 7.35 (d, 2H, J = 8.5 Hz), 7.60 (s, 1H); HRMS (EI) m/z calcd $C_{19}H_{16}N_2O_3SCl_2$ (M^+) 422.0259, found 422.0259.

2.8.8. 3-((Z)-5-(3-chloro-5-ethoxy-4-hydroxybenzylidene)-3-methyl-4-oxothiazolidin-2-ylideneamino)benzoic acid (HL008)

In the same manner as described for HL005. mp 282–283 °C; ^{1}H NMR (DMSO-d_6, 500 MHz): δ 1.31 (t, 3H, J = 7.0 Hz), 3.31 (s, 3H), 4.07 (q, 2H, J = 7.0 Hz), 7.05 (d, 1H, J = 1.7 Hz), 7.14 (d, 1H, J = 1.7 Hz), 7.23 (d, 1H, J = 7.8 Hz), 7.55 (t, 1H, J = 7.8 Hz), 7.56 (t, 1H, J = 1.6 Hz), 7.66 (s, 1H), 7.77 (d, 2H, J = 7.8 Hz); EI-MS m/z 432 (M^+, 100%); HRMS (EI) m/z calcd $C_{20}H_{17}N_2O_5SCl$ (M^+) 432.0547, found 432.0547.

3. Results and discussion

3.1. HL005 was a selective PPARγ ligand

Through random screening, 5-((Z)-5-(3-chloro-5-ethoxy-4-hydroxybenzylidene)-3-methyl -4-oxothiazolidin-2-ylideneamino)-2-chlorobenzoic acid (HL005) from our compound library was found as a selective PPARγ ligand based on SPR assay. The SPR-based Biacore 3000 (Biacore AB, Rapsgatan 7, S-754 50 Uppsala, Sweden) biosensor was used to measure the binding affinity of HL005 with PPARγ-LBD. The PPARγ protein was immobilized on sensor chip, and binding responses in RUs were continuously recorded and presented graphically as a function of time in sensorgrams (Fig. 1). The association of compound with PPARs-LBD were evaluated using the equilibrium dissociation constant (K_D) by fitting the sensorgram with a 1:1 (Langmuir) binding fit model. As shown in Fig. 1A and Table 1, HL005 has a high binding affinity towards PPARγ-LBD, the RU value increased with the increasing concentration of HL005 and the K_D value was fitting as 0.21 μM. In order to inspect the potential

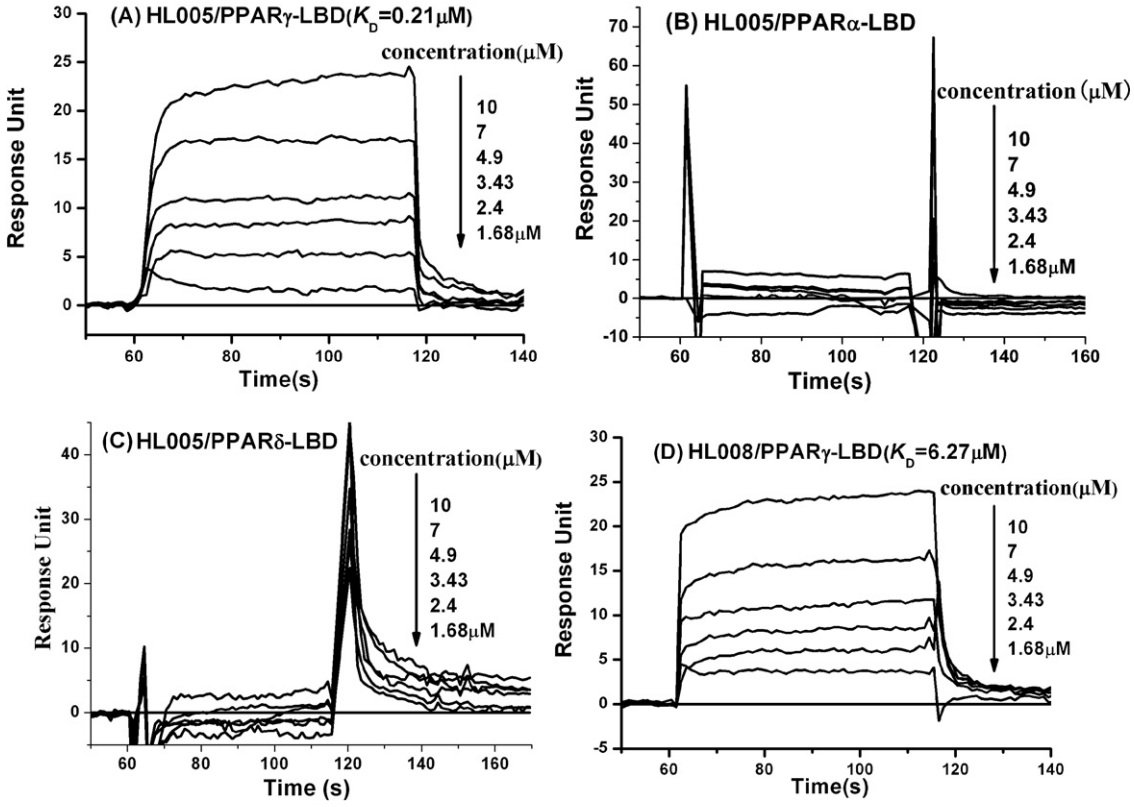

Fig. 1. HL005 specifically binds to PPARγ-LBD as demonstrated by SPR-experiment. The sensorgrams were obtained from injections of series of concentration of HL005 over the immobilized PPARγ-LBD (A), PPARα-LBD (B) or PPARδ-LBD (C) surface. The ligands were injected for 120 s, and dissociation was monitored for more than 2 min. The concentrations (μM) are shown next to the arrows.

binding specificity of this compound, we examined HL005 effect on all three PPAR isoforms. The PPARα-LBD and PPARδ-LBD were expressed and purified as mentioned in "Section 2". The proteins were immobilized on CM5 sensorchip respectively, being similar to PPARγ-LBD. However, when different concentrations of HL005 flow through the sensorchip, it was interesting to see no binding affinity against PPARα-LBD and PPARδ-LBD even at high concentrations (Fig. 1B and C), which suggest HL005 might be a selective PPARγ ligand. In order to get more binding information, a series compounds HL006–HL008 were synthesized and tested. Different concentrations of compounds HL006 and HL007 flow through the sensorchip showed no binding affinity against PPARγ-LBD even at high concentrations. While HL008 showed a less binding affinity (K_D = 6.27 μM) against the protein if we kept the carboxylic substitution and changed chlorine group to hydrogen (Fig. 1D and Table 1).

3.2. HL005 was a PPARγ antagonist

To obtain more detailed information about the activation of HL005–HL008 on PPARγ, a yeast two-hybrid system was constructed. The PPARγ-LBD and the central domain of CBP were cloned in-frame into the vectors pGBKT7 and pGADT7, respectively. After co-transforming the two plasmids into yeast strain AH109, the PPARγ/CBP interactions were evaluated through conducting a convenient α-galactosidase assay based on the expression of MEL1 reporter gene [35]. As shown in Fig. 2, the reported gene expression was stimulated after the addition of rosiglitazone, while HL005 could efficiently antagonized the rosiglitazone (10 μM) stimulated PPARγ/CBP interaction with and IC_{50} of 7.97 μM, and HL008 showed a less antagonist activity with an IC50 of 19.6 μM, while HL006 and HL007 still did not show any activity.

3.3. HL005 inhibited proliferation of MCF-7 and caused cell cycle arrest at G2/M phase

Since many reports show that PPARγ had been developed as an essential target for exploring potential anti-cancer agents, MTT assay was applied to test the inhibition of the above four compounds HL005–HL008 against the proliferation of HCT-116, Du-145, H446, HeLa, PNAC-1, HepG2, Tca-8118, Ls-174, MCF-7 and ZR-75-30 cancer cells. As indicated in Table 2, in all four compounds, only HL005 and HL008 showed inhibition activities against the proliferation of breast cancer cells, the activity of HL008 is less than HL005. The results indicated the specific anti-tumor function of HL005 in breast cancer cell lines, especially for MCF-7 (IC_{50} = 108 μM) cell line (Fig. 3A).

In order to further investigate the HL005-mediated MCF-7 cell growth inhibition, we examined the cell cycle distribution and apoptosis of HL005-treated MCF-7 cells by flow cytometry. The results showed that HL005 could induce apoptosis and cell cycle

Table 2
Compounds' cellular proliferation activity (IC_{50} values, μM).

Cell lines	HL005	HL006	HL007	HL008
HCT-116	NA	NA	NA	NA
Du-145	NA	NA	NA	NA
H446	NA	NA	NA	NA
HeLa	NA	NA	NA	NA
PNAC-1	NA	NA	NA	NA
HepG2	NA	NA	NA	NA
Tca-8118	NA	NA	NA	NA
Ls-174	NA	NA	NA	NA
MCF-7	108	NA	NA	>200
ZR-75-30	>200	NA	NA	>200

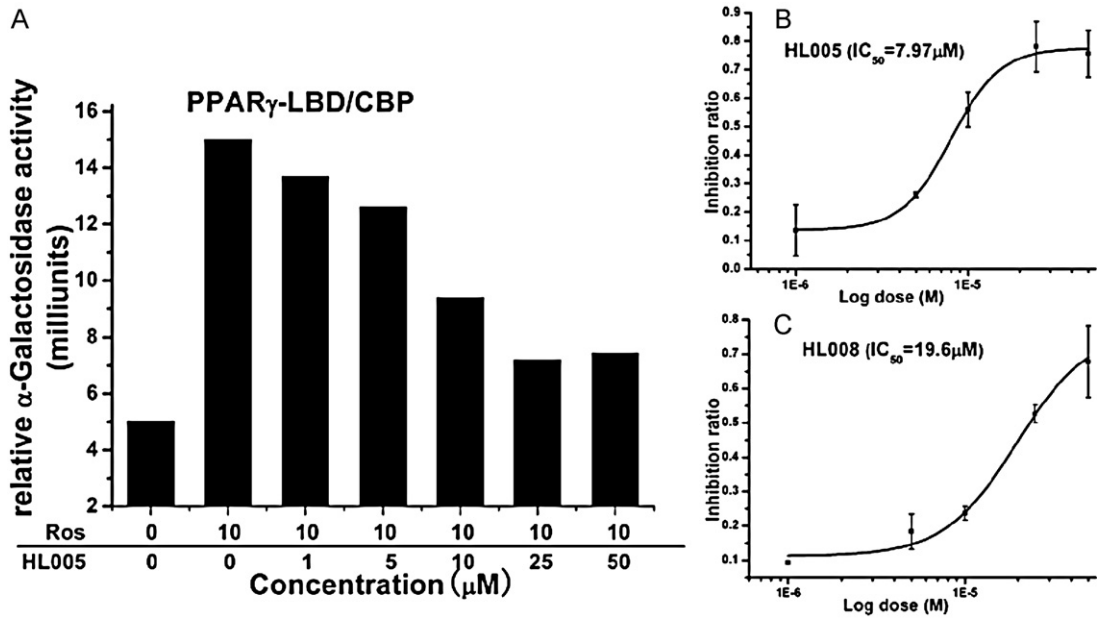

Fig. 2. HL005 inhibits the rosiglitazone-induced PPARγ/CBP interaction in yeast-two hybrid assay. The yeast strain AH109 was co-transfected with pGADT7-CBP and pGBKT7-PPARγ plasmids, then incubated with 10 μM rosiglitazone and different concentrations of HL005. (A) HL005 can antagonisted the stimulation induced by 10 μM rosiglitazone. (B) The fitting IC_{50} value of HL005 against the stimulation induced by rosiglitazone. (C) The fitting IC_{50} value of HL008 against the stimulation induced by rosiglitazone.

arrest at G2/M phase of MCF-7 cell (Fig. 3B and C). After HL005 treatment, cell population in G1 phase decreased from 78.31% in non-treated control cells to 68.97%, and G2/M phase cells increased from 5.31% (control) to 21.52%. The apoptosis induced by HL005 was examined by Annexin V–FITC staining. Fig. 3D showed that the PPAR-γ specific antagonist HL005 can induce the MCF-7 apoptosis at 100 μM. All the above results suggested that HL005 could specifically inhibit the cell growth of MCF-7 by arresting the cell cycle at G2/M phase.

From the MTT result, we found that our PPARγ antagonist – HL005 could affect the breast cancer cell growth, especially for MCF-7. Since large evidence showed that estrogen receptor α (ERα) was dominantly expressed in the human MCF-7 breast cancer cell line, played an important role in the development of breast cancer [36], and ERα could bind to PPAR response element and repressed its transactivation [37]. But use our reported method [38], compounds HL005–HL008 did not show any activities as ER ligand. Accumulating evidence exists on the overexpression of PPARγ in

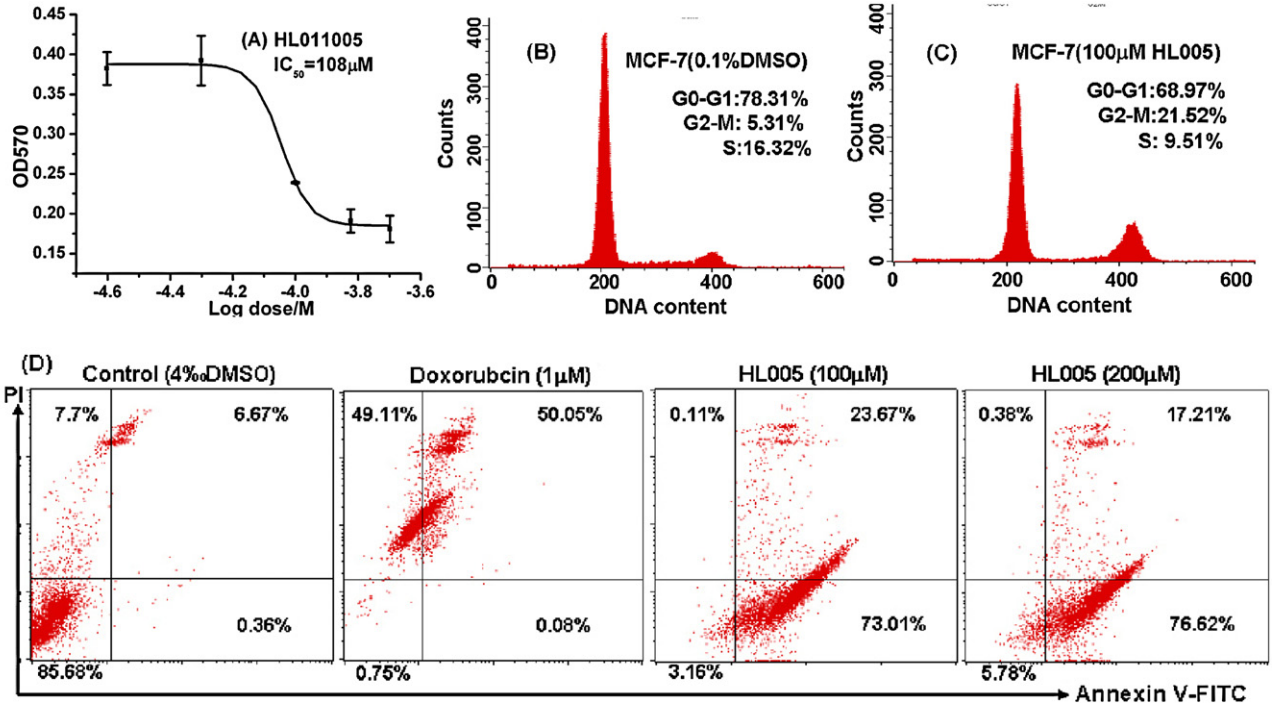

Fig. 3. Induction of cell cycle arrest and apoptosis in MCF-7 cancer cell by HL005. (A) The fitting IC_{50} value of HL005 against MCF-7 cancer cell. Cells were incubated without (B) and with HL005 (C) for 48 h, and then collected, fixed, stained with propidium iodide and analyzed for DNA content by flow cytometry. Percentages of cells in different phases of cell cycle: G1, G2, S and sub-G1 are indicated in each panel. The *X*-axis means DNA content, and the figure is a representative of three independent experiments. (D) Effect of HL005 on apoptosis of MCF-7 cell. DMSO and doxorubcin worked as controls. Apoptosis was measured by Annexin V/PI staining and flow cytometry.

many tumor cells, yet, the biological significance of its role in cancer remains controversial. Activation of this receptor leads to both tumor suppressive and promoting responses based on the set of conditions encountered [39]. The different anticancer activities of HL005 might be attributing to different cellular internal environments of our test cancer cell line.

The obvious study found that the growth inhibition induced by PPARγ agonists or antagonists are media by various mechanisms, either involvement of PPARγ or a PPARγ-independent effect. Such as PPARγ antagonists (T0070907 and GW9662) caused a lack of adhesion and morphologic changes prior to their commitment to apoptosis, which associated with decreased focal adhesion kinase (FAK) activation in hepatocellular and squamous carcinoma cell lines [24,26]. While in esophageal cell line, T0070907 and GW9662 could induce loss of invasion at low concentrations (<10 μM), but could inhibit cell growth and induce apoptosis at high concentrations (>50 μM) [25]. The other PPARγ antagonist – BADGE could induce apoptosis in HCT-116 cell line in a PPARγ-independent manner and that BADGE-induced apoptosis was mediated in caspase-dependent and caspase-independent manners [40]. The apoptosis induced by HL005 might be similar to BADGE which was mediated in caspase-dependent and caspase-independent manners, but different from T0070907 and GW9662, because we did not observe cells lacking adhesion in our assay. The underlying mechanism of HL005 activate biochemical pathways leading to apoptosis is not yet fully enlightened, further studies are under way to determine it.

3.4. Molecular modeling of binding models

Molecular modeling was used to get more binding information between HL005 and PPARγ. The docked pose (orientation and conformation) of HL005 to PPARγ-LBD were schematically presented in Fig. 4. The interactions between HL005 and the active site of PPARγ-LBD formed a U-shaped conformation, carboxylic acid group of HL005 formed five hydrogen bonds with residues Glu286, Ser289, His323, His449 and Tyr473 of PPARγ, which fixed the conformation of HL005 carboxylic acid group among the participating amino acids. That was also the reason why HL006 and HL007 lose the binding affinities. This indicated that carboxylic acid was a critic pharmacophore for designing more potent PPARγ binders. Next to the carboxylic acid group, the benzene ring with chlorine of HL005 was positioned in the hydrophobic region formed by Phe363, Glu286, Phe282, Leu469. The other hydrophobic tail of HL005 occupied the large hydrophobic pocket of PPARγ through hydrophobic contacted with several lipophilic residues, such as Cys285, Leu330, Ile341, Met348 and Met364. This hydrogen bonding patterns we got from the molecular modeling was conserved in most PPARγ–ligand complex structures and is essential for the activity of the ligand.

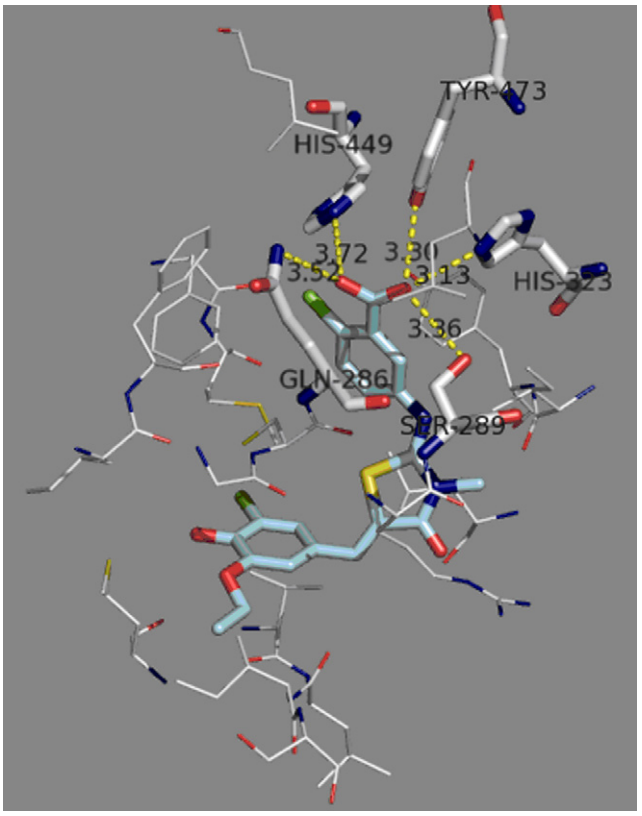

Fig. 4. Stereoview of the binding mode of HL005 at the binding site of PPARγ-LBD with residues around the docked pose within 4.0 Å. Hydrophobic residues in the binding site are shown in line and labeled residues forming hydrogen bonds with HL005 are shown as stick. The coloring for HL005 is as follows: carbon atoms, cyan; oxygen atoms, red; nitrogen atoms, blue; sulfur atoms, yellow; chlorine, green; respectively. Hydrogen atoms have been omitted for clarity. Hydrogen-bonds are represented by yellow dotted lines. All structure figures were prepared using PyMol (http://pymol.sourceforge.net/). (For interpretation of the references to color in this figure legend, the reader is referred to the web version of the article.)

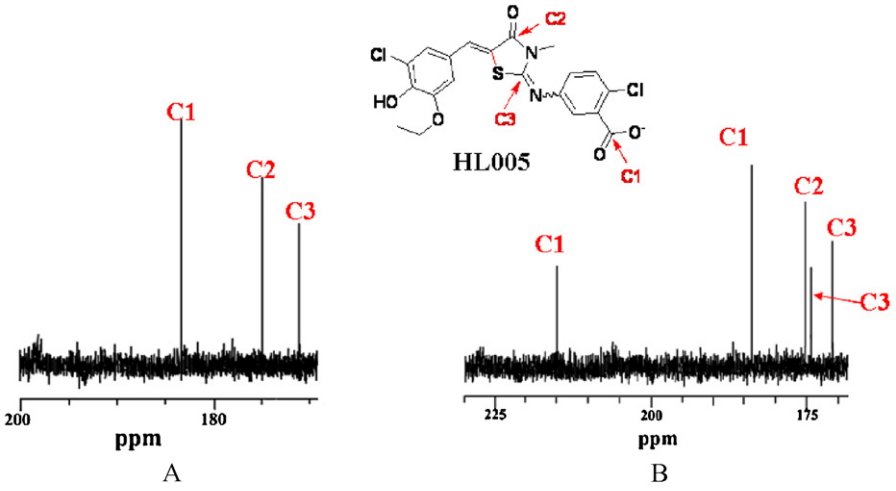

Fig. 5. Expanded room temperature ^{13}C NMR (D_2O) spectra of sodium salt of HL005 (A) and sodium salt of HL005–PPARγ-LBD complex (B). After the addition of PPARγ-LBD, the carboxylic acid of HL005 shifted downfield significantly (marked as C1, the two signals of C1 belong to the unbound and bound types, and same to the C3 signals), C3 shifted downfield a little bit because of the conjugate action with C1, while C2 almost kept the same chemical shift as before the addition of protein.

We could found, consistent with the above SPR results, if the carboxylic acid group was kept in the compound (shown as HL008), the compound could still keep a high binding affinity with a K_D of 6.27 μM. If changed the carboxylic acid head and still keep the chlorine atom on benzene ring (HL006 and HL007), the compound could not bound with protein no longer. These results suggest that carboxylic acid might play an important role in the interaction between these type ligand and PPARγ. In order to verify this interaction, we run the ^{13}C NMR experiments of sodium salt of HL005 both with and without PPARγ.

3.5. Carboxylic acid of HL005 is important in the interaction with PPARγ

The NMR experiment was used to evaluate the binding mode between HL005 and PPARγ. The carbon resonance of **C1** (carboxylic acid for HL005) appeared at 183.2 ppm in the ^{13}C NMR spectrum (Fig. 5A), while from Fig. 5B, we could find the resonance of **C1** shifted downfield from 182.7 ppm to 215.5 ppm after the addition of PPARγ. Compared with Fig. 3A and B, we found that after bound with PPARγ, besides the resonance of **C1**, **C3** (the carbon atom which conjugated with the carboxylic acid) also shifted downfield because of the conjugate action. While the chemical shift of **C2** did not show any observable change because this carbon atom was far away from the carboxylic acid and had no conjugate action with carboxylic acid. It also showed that the carboxylic acid of HL005 worked as hydrogen bond acceptor and contributed a strong interaction with polarity groups of PPARγ.

4. Conclusions

More recently, based on both in vitro and in vivo studies, perturbation of PPARγ expression and activity had been suggested as a therapeutic strategy for several epithelial tumour types, including breast cancer, lung, prostate and bladder [1,22,41–44]. Understanding the involvement and role of PPARγ in tumour growth inhibition has important implications for both interpreting the results of current clinical trials [45] and the pharmacology of such compounds.

In our work, we are interested in finding a new type of small molecules to work as a selective binding ligand for PPARγ, Biacore 3000 results based on surface plasmon resonance (SPR) technique clearly showed the HL005 has a highly specific binding affinity towards PPARγ with the K_D = 0.21 μM. The molecular docking result and ^{13}C NMR spectra showed that the carboxylic acid of the compound played an important role when HL005 bound with PPARγ. As a new PPARγ antagonist, HL005 could strongly antagonize the rosiglitazone-induced recruitment of the coactivator for PPARγ (IC_{50} = 7.97 μM) in our yeast two hybrid.

There are preclinical in vivo data showed that PPARγ antagonists can be administered safely, with favorable metabolic effects as well as antitumor effects, and PPARγ antagonists represented a new drug class that holds promise as a broadly application for cancer treatment [46]. We test the anticancer activity of HL005 – a new PPARγ antagonist. All the cell lines used in this study were reported can express PPARγ protein. But interesting, HL005 could only specially inhibit the proliferation of MCF-7 cell line in a concentration-dependent manner, induced cell apoptosis and arrested cell cycle at G2/M phase.

There are many PPARγ ligands showing antitumor activity in various preclinical models of breast cancer or other malignancies, the molecular targets of PPARγ ligands in cancer cells are still poorly defined, and many of the anticancer effects of PPARγ ligands are probably not media by PPARγ [47]. Although, the extra role of PPARγ on carcinogenesis and tumor cell growth is still controversial because of the many conflicting reports that variably provide evidence for tumor suppressor or promoter role, PPARγ antagonists still could be considered as important candidates for further development as anticancer agents, and the best drug or drug combination need to be well established.

Acknowledgements

This work was supported by Shanghai Pujiang Program (D type, Grant PJ200700247), the Innovation Program of Shanghai Municipal Education Commission (Grant 10ZZ41), the Shanghai Committee of Science and Technology (Grant 08JC1407800), the National Natural Science Foundation of China (Grants 90813005 and 10979072), the 111 Project (Grant B07023) and the 863 Hi-Tech Program of China (Grant 2007AA02Z147).

References

[1] S. Han, J. Roman, Peroxisome proliferator-activated receptor gamma: a novel target for cancer therapeutics? Anticancer Drugs 18 (3) (2007) 237–244.
[2] J.M. Keller, P. Collet, A. Bianchi, C. Huin, P. Bouillaud-Kremarik, P. Becuwe, H. Schohn, L. Domenjoud, M. Dauca, Implications of peroxisome proliferator-activated receptors (PPARS) in development, cell life status and disease, Int. J. Dev. Biol. 44 (5) (2000) 429–442.
[3] M. Lehrke, M.A. Lazar, The many faces of PPARgamma, Cell 123 (6) (2005) 993–999.
[4] U. Kintscher, R.E. Law, PPARgamma-mediated insulin sensitization: the importance of fat versus muscle, Am. J. Physiol. Endocrinol. Metab. 288 (2) (2005) E287–E291.
[5] G. Chinetti, S. Griglio, M. Antonucci, I.P. Torra, P. Delerive, Z. Majd, J.C. Fruchart, J. Chapman, J. Najib, B. Staels, Activation of proliferator-activated receptors alpha and gamma induces apoptosis of human monocyte-derived macrophages, J. Biol. Chem. 273 (40) (1998) 25573–25580.
[6] S. Kersten, B. Desvergne, W. Wahli, Roles of PPARs in health and disease, Nature 405 (6785) (2000) 421–424.
[7] D.J. Mangelsdorf, C. Thummel, M. Beato, P. Herrlich, G. Schutz, K. Umesono, B. Blumberg, P. Kastner, M. Mark, P. Chambon, R.M. Evans, The nuclear receptor superfamily: the second decade, Cell 83 (6) (1995) 835–839.
[8] D. Panigrahy, S. Huang, M.W. Kieran, A. Kaipainen, PPAR gamma as a therapeutic target for tumor angiogenesis and metastasis, Cancer Biol. Ther. 4 (7) (2005) 687–693.
[9] R.K. Semple, V.K. Chatterjee, S. O'Rahilly, PPAR gamma and human metabolic disease, J. Clin. Invest. 116 (3) (2006) 581–589.
[10] N. Takahashi, T. Okumura, L. Motomura, Y. Fujimoto, I. Kawabata, Y. Kohgo, Activation of PPAR gamma inhibits cell growth and induces apoptosis in human gastric cancer cells, FEBS Lett. 455 (1–2) (1999) 135–139.
[11] M.B. Sporn, N. Suh, D.J. Mangelsdorf, Prospects for prevention and treatment of cancer with selective PPAR gamma modulators (SPARMs), Trends Mol. Med. 7 (9) (2001) 395–400.
[12] T. Kubota, K. Koshizuka, E.A. Williamson, H. Asou, J.W. Said, S. Holden, I. Miyoshi, H.P. Koeffler, Ligand for peroxisome proliferator-activated receptor gamma (troglitazone) has potent antitumor effect against human prostate cancer both in vitro and in vivo, Cancer Res. 58 (15) (1998) 3344–3352.
[13] F. Yin, S. Wakino, Z. Liu, S. Kim, W.A. Hsueh, A.R. Collins, A.J. Van Herle, R.E. Law, Troglitazone inhibits growth of MCF-7 breast carcinoma cells by targeting G1 cell cycle regulators, Biochem. Biophys. Res. Commun. 286 (5) (2001) 916–922.
[14] M. Kato, T. Kusumi, S. Tsuchida, M. Tanaka, M. Sasaki, H. Kudo, Induction of differentiation and peroxisome proliferator-activated receptor gamma expression in colon cancer cell lines by troglitazone, J. Cancer Res. Clin. Oncol. 130 (2) (2004) 73–79.
[15] K. Ohta, T. Endo, K. Haraguchi, J.M. Hershman, T. Onaya, Ligands for peroxisome proliferator-activated receptor gamma inhibit growth and induce apoptosis of human papillary thyroid carcinoma cells, J. Clin. Endocrinol. Metab. 86 (5) (2001) 2170–2177.
[16] V.G. Keshamouni, R.C. Reddy, D.A. Arenberg, B. Joel, V.J. Thannickal, G.P. Kalemkerian, T.J. Standiford, Peroxisome proliferator-activated receptor-gamma activation inhibits tumor progression in non-small-cell lung cancer, Oncogene 23 (1) (2004) 100–108.
[17] A.P. Heaney, M. Fernando, S. Melmed, PPAR-gamma receptor ligands: novel therapy for pituitary adenomas, J. Clin. Invest. 111 (9) (2003) 1381–1388.
[18] N.B. Mettu, T.B. Stanley, M.A. Dwyer, M.S. Jansen, J.E. Allen, J.M. Hall, D.P. McDonnell, The nuclear receptor-coactivator interaction surface as a target for peptide antagonists of the peroxisome proliferator-activated receptors, Mol. Endocrinol. 21 (10) (2007) 2361–2377.
[19] P.L. Feldman, M.H. Lambert, B.R. Henke, PPAR modulators and PPAR pan agonists for metabolic diseases: the next generation of drugs targeting peroxisome proliferator-activated receptors? Curr. Top. Med. Chem. 8 (9) (2008) 728–749.
[20] C. Ulivieri, C.T. Baldari, The potential of peroxisome proliferator-activated receptor gamma (PPARgamma) ligands in the treatment of hematological malignancies, Mini Rev. Med. Chem. 7 (9) (2007) 877–887.

[21] C.E. Clay, G. Atsumi, K.P. High, F.H. Chilton, Early de novo gene expression is required for 15-deoxy-delta(12,14)-prostaglandin J(2)-induced apoptosis in breast cancer cells, J. Biol. Chem. 276 (50) (2001) 47131–47135.
[22] E. Elstner, C. Muller, K. Koshizuka, E.A. Williamson, D. Park, H. Asou, P. Shintaku, J.W. Said, D. Heber, H.P. Koeffler, Ligands for peroxisome proliferator-activated receptorgamma and retinoic acid receptor inhibit growth and induce apoptosis of human breast cancer cells in vitro and in BNX mice, Proc. Natl. Acad. Sci. U.S.A. 95 (15) (1998) 8806–8811.
[23] J.K. Hampel, L.M. Brownrigg, D. Vignarajah, K.D. Croft, A.M. Dharmarajan, J.M. Bentel, I.B. Puddey, B.B. Yeap, Differential modulation of cell cycle, apoptosis and PPARgamma2 gene expression by PPARgamma agonists ciglitazone and 9-hydroxyoctadecadienoic acid in monocytic cells, Prostaglandins Leukot. Essent. Fatty Acids 74 (5) (2006) 283–293.
[24] T. Masuda, K. Wada, A. Nakajima, M. Okura, C. Kudo, T. Kadowaki, M. Kogo, Y. Kamisaki, Critical role of peroxisome proliferator-activated receptor gamma on anoikis and invasion of squamous cell carcinoma, Clin. Cancer Res. 11 (11) (2005) 4012–4021.
[25] H. Takahashi, K. Fujita, T. Fujisawa, K. Yonemitsu, A. Tomimoto, I. Ikeda, M. Yoneda, T. Masuda, K. Schaefer, L.J. Saubermann, T. Shimamura, S. Saitoh, M. Tachibana, K. Wada, H. Nakagama, A. Nakajima, Inhibition of peroxisome proliferator-activated receptor gamma activity in esophageal carcinoma cells results in a drastic decrease of invasive properties, Cancer Sci. 97 (9) (2006) 854–860.
[26] K.L. Schaefer, K. Wada, H. Takahashi, N. Matsuhashi, S. Ohnishi, M.M. Wolfe, J.R. Turner, A. Nakajima, S.C. Borkan, L.J. Saubermann, Peroxisome proliferator-activated receptor gamma inhibition prevents adhesion to the extracellular matrix and induces anoikis in hepatocellular carcinoma cells, Cancer Res. 65 (6) (2005) 2251–2259.
[27] J. Sambrook, M.J. Gething, Protein structure. Chaperones, paperones, Nature 342 (6247) (1989) 224–225.
[28] G. Harris, R.A. Ghazallah, D. Nascene, B. Wuertz, F.G. Ondrey, PPAR activation and decreased proliferation in oral carcinoma cells with 4-HPR, Otolaryngol. Head Neck Surg. 133 (5) (2005) 695–701.
[29] R.T. Nolte, G.B. Wisely, S. Westin, J.E. Cobb, M.H. Lambert, R. Kurokawa, M.G. Rosenfeld, T.M. Willson, C.K. Glass, M.V. Milburn, Ligand binding and co-activator assembly of the peroxisome proliferator-activated receptor-gamma, Nature 395 (6698) (1998) 137–143.
[30] M. Rarey, B. Kramer, T. Lengauer, G. Klebe, A fast flexible docking method using an incremental construction algorithm, J. Mol. Biol. 261 (3) (1996) 470–489.
[31] S.J. Weiner, P.A. Kollman, D.T. Nguyen, D.A. Case, An all atom force field for simulations of proteins and nucleic acids, J. Comput. Chem. 7 (2) (1986) 230–252.
[32] J. Sadowski, J. Gasteiger, From atoms and bonds to three-dimensional atomic coordinates: automatic model builders, Chem. Rev. 93 (7) (1993) 2567–2581.
[33] D. Albanese, M. Penso, Synthesis of isothiocyanates by reaction of amides with carbon disulfide in the presence of solid potassium carbonate/sodium hydroxide mixture, Synthetics 11 (1991) 1001–1002.
[34] D.H. Hua, X. Huang, Y. Chen, S.K. Battina, M. Tamura, S.K. Noh, S.I. Koo, I. Namatame, H. Tomoda, E.M. Perchellet, J.P. Perchellet, Total syntheses of (+)-chloropuupehenone and (+)-chloropuupehenol and their analogues and evaluation of their bioactivities, J. Org. Chem. 69 (18) (2004) 6065–6078.
[35] Q. Chen, J. Chen, T. Sun, J.H. Shen, X. Shen, H.L. Jiang, A yeast two-hybrid technology-based system for the discovery of PPAR gamma agonist and antagonist, Anal. Biochem. 335 (2) (2004) 253–259.
[36] W.J. Welboren, F.C. Sweep, P.N. Span, H.G. Stunnenberg, Genomic actions of estrogen receptor alpha: what are the targets and how are they regulated? Endocr. Relat. Cancer 16 (4) (2009) 1073–1089.
[37] D. Bonofiglio, S. Gabriele, S. Aquila, S. Catalano, M. Gentile, E. Middea, F. Giordano, S. Ando, Estrogen receptor alpha binds to peroxisome proliferator-activated receptor response element and negatively interferes with peroxisome proliferator-activated receptor gamma signaling in breast cancer cells, Clin. Cancer Res. 11 (17) (2005) 6139–6147.
[38] J. Shen, C. Tan, Y. Zhang, X. Li, W. Li, J. Huang, X. Shen, Y. Tang, Discovery of potent ligands for estrogen receptor beta by structure-based virtual screening, J. Med. Chem. 53 (14) (2010) 5361–5365.
[39] A. Krishnan, S.A. Nair, M.R. Pillai, Biology of PPAR gamma in cancer: a critical review on existing lacunae, Curr. Mol. Med. 7 (6) (2007) 532–540.
[40] S. Fehlberg, S. Trautwein, A. Goke, R. Goke, Bisphenol A diglycidyl ether induces apoptosis in tumour cells independently of peroxisome proliferator-activated receptor-gamma, in caspase-dependent and -independent manners, Biochem. J. 362 (3) (2002) 573–578.
[41] G.L. Rubin, Y. Zhao, A.M. Kalus, E.R. Simpson, Peroxisome proliferator-activated receptor gamma ligands inhibit estrogen biosynthesis in human breast adipose tissue: possible implications for breast cancer therapy, Cancer Res. 60 (6) (2000) 1604–1608.
[42] S.J. Roberts-Thomson, Peroxisome proliferator-activated receptors in tumorigenesis: targets of tumour promotion and treatment, Immunol. Cell Biol. 78 (4) (2000) 436–441.
[43] X. Wang, M.W. Kilgore, Signal cross-talk between estrogen receptor alpha and beta and the peroxisome proliferator-activated receptor gamina1 in MDA-MB-231 and MCF-7 breast cancer cells, Mol. Cell. Endocrinol. 194 (1–2) (2002) 123–133.
[44] G.M. Pighetti, W. Novosad, C. Nicholson, D.C. Hitt, C. Hansens, A.B. Hollingsworth, M.L. Lerner, D. Brackett, S.A. Lightfoot, J.M. Gimble, Therapeutic treatment of DMBA-induced mammary tumors with PPAR ligands, Anticancer Res. 21 (2A) (2001) 825–829.
[45] H.J. Burstein, G.D. Demetri, E. Mueller, P. Sarraf, B.M. Spiegelman, E.P. Winer, Use of the peroxisome proliferator-activated receptor (PPAR) gamma ligand troglitazone as treatment for refractory breast cancer: a phase II study, Breast Cancer Res. Treat. 79 (3) (2003) 391–397.
[46] J.D. Burton, D.M. Goldenberg, R.D. Blumenthal, Potential of peroxisome proliferator-activated receptor gamma antagonist compounds as therapeutic agents for a wide range of cancer types, PPAR Res. (2008) 494161, doi:10.1155/2008/494161.
[47] M.H. Fenner, E. Elstner, Peroxisome proliferator-activated receptor-gamma ligands for the treatment of breast cancer, Expert Opin. Investig. Drugs 14 (6) (2005) 557–568.